water

MDPI

Article

Multivariate Chemometric Analysis of Membrane Fouling Patterns in Biofilm Ceramic Membrane Bioreactor

Olga Kulesha [1,2,*], Zakhar Maletskyi [1] and Harsha Ratnaweera [1]

[1] Faculty of Science and Technology (REALTEK), Norwegian University of Life Sciences, P.O. Box 5003, 1432 Aas, Norway; zakhar.maletskyi@nmbu.no (Z.M.); harsha.ratnaweera@nmbu.no (H.R.)

[2] Department of General and Inorganic Chemistry, Faculty of Chemical Technology, National Technical University of Ukraine "Igor Sikorsky Kyiv Polytechnic Institute", Peremohy 37, 03056 Kyiv, Ukraine

* Correspondence: olga.kulesha@nmbu.no; Tel.: +47-406-755-92

Received: 27 June 2018; Accepted: 22 July 2018; Published: 26 July 2018

Abstract: Membrane fouling highly limits the development of Membrane bioreactor technology (MBR), which is among the key solutions to water scarcity. The current study deals with the determination of the fouling propensity of filtered biomass in a pilot-scale biofilm membrane bioreactor to enable the prediction of fouling intensity. The system was designed to treat domestic wastewater with the application of ceramic microfiltration membranes. Partial least squares regression analysis of the data obtained during the long-term operation of the biofilm-MBR (BF-MBR) system demonstrated that Mixed liquor suspended solids (MLSS), diluted sludge volume index (DSVI), chemical oxygen demand (COD), and their slopes are the most significant for the estimation and prediction of fouling intensity, while normalized permeability and its slope were found to be the most reliable fouling indicators. Three models were derived depending on the applied operating conditions, which enabled an accurate prediction of the fouling intensities in the system. The results will help to prevent severe membrane fouling via the change of operating conditions to prolong the effective lifetime of the membrane modules and to save energy and resources for the maintenance of the system.

Keywords: water crisis; biofilm membrane bioreactor; membrane fouling; operation; ceramic membranes; multivariate statistics

1. Introduction

The World Economic Forum (WEF) includes water crises in the group of risks with the highest likelihood and impact, which are strongly interconnected with the trends in climate change that can degrade the environment and cause food crises [1]. According to the WEF, the main reason for a water crisis is a significant decline in the available quality and quantity of fresh water, thus resulting in harmful effects to human health and economic activity. Competition for water between agriculture, industry and municipal supply is being complicated by political tension around water in stressed regions, thus leading to the future shock of so-called "grim reaping" [2].

Water reuse is gaining momentum as a reliable alternative source of freshwater in the face of growing water demand, which is shifting the paradigm of wastewater management from "disposal" to "reuse and resource recovery" [3]. Growing globally [4], water reuse plays a key role in bringing significant environmental, social and economic benefits [5]. Advanced tertiary treatment is a rule of thumb in water reuse and is an important factor of system resilience in the case of wastewater reuse as a part of a decentralized water supply [6]. However, of all the wastewater produced worldwide, only a very small fraction actually undergoes tertiary treatment [3]. Efficient, reliable, sustainable and

economically feasible technologies are highly demanded when it comes to potential cost recovery by treating wastewater to a water quality standard acceptable to users.

Membrane bioreactor technology (MBR) is a highly competitive technology when applied in water reuse schemes. It provides excellent nutrient removal efficiency, compactness, complete biomass retention with no use of a secondary clarifier, and produces a low carbon footprint [7–9]. Additionally, strengthening requirements for reclaimed water quality is expected to drive the MBR market to USD 8.27 billion by 2025 [10].

However, membrane fouling is the main restraint to further penetration of MBR into cost-sensitive markets, including the water reuse market in small communities and developing countries, which is primarily due to the occurrence of unplanned high operating costs [11–14]. Several approaches to detect, control and prevent membrane fouling in MBR have been developed during the last decades, focusing on pre-treatment or modification of mixed liquor, membrane properties, operating conditions, etc. [15–19]. Considering the pros and cons of the aforementioned, there is no unified approach to dealing with membrane fouling.

Several types of research demonstrated that a combination of two or more fouling prevention factors gives the best practical results through the synergy of anti-fouling mechanisms [20–22]. Therefore, the current research considers the use of a combination of biofilm-MBR (BF-MBR) process configuration with the application of ceramic flat-sheet membranes.

BF-MBR combines membrane separation, biological contact oxidation and fluidized bed wastewater treatment (as in the moving-bed-biofilm reactor (MBBR) process). This results in better effluent quality due to reliable degradation of organics and nutrients, a lower sludge production rate and a smaller footprint, together with stable and reliable operation, strong resistance to shock loading, and adaptability due to high biomass concentration and diversity in bacterial population [23]. The BF-MBR process has demonstrated lower membrane fouling rates and better settling ability of suspended biomass than in conventional MBR and MBBR processes separately [12,24].

In another study [25], porous suspended biofilm carriers were introduced to a submerged ceramic membrane bioreactor to explore their effectiveness in membrane flux enhancement. Alleviation of membrane fouling, in this case, is anticipated via mechanical scouring of the cake layer on the membrane surface and modification of mixed liquor characteristics. It has been shown that a combination of biofilm carriers with the ceramic membrane in MBR leads to 2.7 times lower cake resistance and 1.5 times lower total resistance.

Mixed liquor suspended solids (MLSS), chemical oxygen demand (COD) and sludge relative hydrophobicity (RH) are among the main characteristic parameters of activated sludge suspension that are traditionally monitored in an MBR system [22,26–31].

MLSS provides information about mixed liquor fouling propensity, apart from indicating a biomass potential to decompose wastewater impurities, determining an aeration tank volume, and affecting the aeration demand and sludge production [28,32]. Several researchers acknowledged there was a complex relationship between MLSS and membrane fouling [9,29,33].

The COD parameter accounts for the organic load and the biological treatment efficiency in terms of the degradation of organic contaminants [34]. In addition, as specified by Le-Clech et al. [29], Ji and Zhou [35], Meng et al. [36], in MBR systems, soluble COD is an indicator of the soluble microbial product (SMP) level. SMP is generally considered to be one of the major foulants in MBR [37–39].

Biomass RH is one of the key parameters used to estimate the resistance caused by microbial aggregates. RH determines flocculation ability of the sludge flocs based on their hydrophobic interactions with each other, which in turn controls their dewaterability [32,40,41]. RH of the activated sludge influences initial biomass attachment to the membrane and, therefore, membrane permeability (i.e., determines whether a membrane can be more or less sensitive to different foulants).

The sludge volume index (SVI)/diluted sludge volume index (DSVI) is another characteristic that is monitored in MBR systems. Although this parameter primarily characterizes the activated sludge settling properties, it is also widely applied in MBRs, since it indicates the flocculation characteristics of

the activated sludge and is associated with filamentous bacteria. The latter induces membrane fouling through the release of SMPs from the sludge flocs, thus increasing their concentration via viscosity increase and by fixing the foulants on the membrane surface, thus forming practically a non-porous cake layer [9,33,42–44].

In general, a number of studies indicated that the above-mentioned biomass characteristics exhibit specific tendencies in influencing fouling in MBR (Table 1).

Table 1. The influence of activated sludge parameters on the biomass fouling propensity.

Parameter	Correlation with the Fouling	Possible Fouling Mechanism	References
MLSS [1]	Positive	Intense cake layer formation on the membrane surface. Increase in the suspension viscosity. Excessive growth of filamentous bacteria. Increase in microbial metabolic products such as SMP [2] and EPS [3], which are the major foulants.	[34,45–51]
MLSS [1]	Negative (irreversible fouling)	MLSS [1] 12–18 g/L: The formed cake layer causes the prevention of the pore blocking development and induces an increased porosity of the cake layer.	[15,45]
COD [4]	Positive	COD [4] in the form of colloids proteins (adsorption mechanism) and other soluble organic fractions, causing irreversible fouling; higher organic load causes an increase in the production of specific EPS [3] and macromolecules in the SMP [2]/EPS [3] fractions, deflocculation of the mixed liquor, and a fast formation of cake layers.	[9,29,35,52–56]
RH [6] (mostly hydrophilic membranes)	Negative	RH [6] increase: Enhanced AS [5] flocculation due to more intense hydrophobic interactions between sludge flocs, resulting in the formation of larger aggregates with less water content, and decreased interaction between the flocs and membrane surface. RH [6] decrease: Floc deterioration.	[57–62]
	Positive	RH [6] increase: A formation of a thin cake layer, promoting the adhesion of proteins and carbohydrates in the form of SMP [2] on the membrane surface and its pores, resulting in irreversible and irrecoverable fouling.	[26,63]
SVI (DSVI) [7]	Positive	High DSVI [7]: Evolution of the flocs to the more irregular rougher shapes which more likely adhere to the surface of the membrane, intertwisting with the fibers. This forms a dense, non-porous cake with large thickness. The possible decrease of the bound protein and release of SMP [2] triggers deflocculation and the increase in fouling intensity.	[64–69]

Notes: [1] Mixed liquor suspended solids; [2] Soluble microbial products; [3] Extracellular polymeric substances; [4] Chemical oxygen demand; [5] Activated sludge; [6] Relative hydrophobicity; [7] Sludge volume index (diluted sludge volume index).

It is worth noting that application of ceramic membranes in MBR started from a niche where polymer membranes either failed or provided insufficient results: The cases when high effluent quality is required or the process depends on ceramic membrane robustness [70]. Compared to their polymeric counterparts, ceramic membranes have the following advantages:

1. Higher mechanical strength and chemical resistance to oxidants and solvents. The modules are backwashable with the possible application of high backwash pressure/flux [71,72] and can withstand much more aggressive operation and chemical cleaning conditions (i.e., can be used in combination with ultrasonic irradiation and undergo a soaking in more concentrated NaClO, NaOH, and acidic solutions). In addition, they can undergo the influence of higher temperatures and pH without damaging the active layer [73–77].
2. Higher hydrophilicity, thus no affinity to organic foulants which are mostly of a hydrophobic nature [70,78,79].

The outcomes are: High permeability recovery [80]; a longer period of operation between the chemical cleanings due to more efficient removal of reversible and irreversible fouling [29,79]; enhanced concentration polarization control; and, higher applicable net permeate fluxes and permeabilities are sustained [81–83], consequently leading to a long lifespan.

Ceramic membranes proved to be an effective and reliable MBR component, leading to higher treatment efficiencies of COD, ammonium, and phosphorus elimination [84,85]. In addition, higher

treatment performance in terms of COD and MLSS removal, more stable operation and less transmembrane pressure (TMP) increase was exhibited by the MBR with ceramic modules, compared to the system with the polymeric units [86]. Lower TMP increase, higher removal of non-purgeable organic compounds and lower UV absorbance of the permeate was demonstrated by Hofs et al. [87] in relation to the surface water samples being treated by ceramic modules.

From an economic point of view, the tremendously higher cost of the application of the MBR systems with the ceramic membranes in comparison to the use of the systems with the polymeric modules is rather a stereotype than a reality at present. According to a study by Park et al. [83], the incorporation of membrane modules into the water treatment plant (WTP) makes up 13% and 24% of the total capital cost for polymeric and ceramic WTP, respectively. The comparative analysis demonstrated that the polymeric WTP (with capacity 30,000 m^3/day) are indeed cheaper in terms of the capital costs than their ceramic counterparts, but the difference is not significant: USD 28,019 vs. USD 32,634, respectively. Moreover, the annual operating expenses of the filtration process are more than twice as high for the polymeric modules (USD 562,717) as for the ceramic modules (USD 217,725). This is mainly due to the membrane replacement costs for polymeric WTP, which constitute 61% of the operational expenses. Low operation costs of the systems with ceramic membranes were also acknowledged by Jin et al. [74]. As specified by Park et al. [83], the assessed life cycle costs (LCC) of water from the ceramic and polymeric membrane WTPs are, USD 0.28/m^3 and USD 0.274/m^3, respectively (at the flux of 41.7 LMH). If fluxes of 63 LMH and higher are applied, the LCC of the produced water decreases for the ceramic membranes, thus increasing their feasibility.

In addition, since the manufacturing of the ceramic membranes is an energy-consuming process, a number of recent studies have successfully developed and evaluated the performance of low-cost ceramic membranes [88–93].

Despite many studies on membrane fouling in general, and on BF-MBR or the application of ceramic membranes in particular, only a few findings that are relevant to detection and control of membrane fouling in submerged ceramic BF-MBR come from a pilot or full-scale product. Nevertheless, understanding, detection, and control of membrane fouling via applying advanced statistics and mathematical modelling represents a significant potential for improvement of the cost-efficiency of the process and provides the instruments for dynamic and real-time process control.

Chemometrics serves as a bridge between the state of a chemical system and its measured characteristics, which enhances the efficiency of automatic control systems. Chemometric analysis is based on the application of mathematical and statistical techniques to improve comprehension of the system properties and to link them to analytical measurements. The modelling of the patterns in the dataset results in model derivation. This model can be further used to predict identical parameters as in the initial model but in application to new data [94]. The following multivariate statistical data analysis methods are commonly used as chemometric tools for the interpretation of the acquired data: Cluster analysis (CA), discriminant analysis (DA), principal component analysis (PCA), partial least squares analysis (PLS), multiple linear regression (MLR), principal component regression (PCR), and partial least squares discriminant analysis (PLS-DA) [94–96].

It is worth mentioning that PLS is an advanced statistical technique due to the applied validation tools, noise elimination, and the ability to determine the independent influence of each input variable, even if there is a collinearity between them [59].

A number of recent studies were devoted to the application of modelling using multivariate data analysis for fouling control in MBR. In the study by Philippe et al. [97], the authors performed a PCA to distinguish a correlation between the operational parameters and the characteristics of filtered biomass in a full-scale municipal MBR. Among all the variables, solids retention time (SRT), MLSS, the food to microorganism ratio (F:M), pH and temperature (T) were found to be representative for describing the fouling behaviour. According to the plot of weighted variables, SRT, MLSS and pH positively contributed to the principal components (PCs) one and two, while the F:M ratio exhibited a negative influence. Temperature has a controversial contribution to the PCs in the model. However, the attained

models managed to predict the development of permeability merely in one membrane tank and failed while applying them at different operation stages for all four membrane tanks in the system.

In the work by Kaneko and Funatsu [98], wastewater temperature, the duration of filtration, water temperature, and the inverse of flux and TMP were inputted into the model. PCA was applied as a visualization tool for the discriminant model. As concluded, the accuracy and the predictive ability of the derived model can be increased if the additional parameters related to the water quality and operating conditions are used.

A similar choice of variables was made in the study by De Temmerman et al. [99], where PCA was based on temperature, flux, TMP slope, and pressure peaks during the filtration and chemically enhanced backwash (CEB) for the full-scale MBR. The detection of the fouling types (reversible/irreversible and irrecoverable) was among the prime research goals. The TMP slope and pressure peak during the filtration were found to have a positive relationship. Meanwhile, they were negatively linked to the temperature and the CEB pressure peak along the PC-1 axis. Along the PC-3 axis, flux exhibited a negative correlation with water temperature and the backwash pressure peak. The variance of the CEB pressure peak was attributed to irrecoverable fouling, while pressure peaks during the filtration were attributed to reversible and irreversible fouling types. However, the scores plot indicated no clear trends.

Partial least squares regression analysis applying leave-one-out cross-validation was performed in the work by Van den Broeck [59] to find the influence of the activated sludge parameters on filterability in industrial and municipal MBRs. A relatively deep analysis of the biomass characteristics was conducted. The content of proteins and polysaccharides, sludge relative hydrophobicity, sludge dissociation constant, mean particle size, and the surface fraction of activated sludge particles equal to 1 pixel were used to predict any change of filtration resistance. An accurate estimation of the filtration resistance was observed, which was characterized by the sum of square errors equal to 0.076 (R-squared = 0.99). However, a number of factors (latent variables) exceeded 9, indicating a complexity of the derived model. As concluded, a combination of chosen activated sludge parameters succeeded in predicting sludge filterability, while, when taken individually, they were poor indicators of the biomass fouling propensity.

Consequently, the following knowledge gaps can be identified: The studies which are focused on the modelling of the relationship between operating parameters and filterability do not typically take into consideration biomass characteristics as potential fouling indicators, despite the fact that these are among the main factors affecting the fouling process [9,100,101]. Meanwhile, those studying the statistical evaluation of the relationship between mixed liquor parameters and biomass fouling propensity do not provide the information on the influence of the operating parameters on the fouling intensity. Most importantly, there is also still a need to study the application of the PLS regression to the processes in the biofilm membrane bioreactor due to the lack of research data. In addition, there is a controversy over the influence of the selected biomass parameters on the fouling intensity (Table 1), whereas the development of a reliable BF-MBR system requires concrete patterns.

Applying PLS analysis, the current work encapsulates the relationship between the mixed liquor characteristics, fouling indicators and the operation conditions in BF-MBR with ceramic modules, and thus provides a comprehensive analysis of the system performance and the mechanisms for influencing it.

The purpose of this research was to develop and validate a PLS regression model based on the mixed liquor characteristics and the indicators of fouling intensity, considering the influence of the operation parameters on the filtration performance in the BF-MBR with ceramic membranes, in order to detect membrane fouling patterns and to develop process control and a fouling mitigation approach.

2. Materials and Methods

In general, this study consists of the acquisition of operational data from a BF-MBR pilot plant at various sets of operating conditions followed by statistical analysis.

The BF-MBR pilot plant had a four-stage design (Figure 1) comprising equalization (I) and treated water (IV) compartments, and a MBBR chamber (II) and a separation chamber (III) with the submerged membranes being in contact with suspended biofilm carriers. Compartments I, II and III were interconnected through overflow, while the separation process from chamber III to chamber IV was driven by a reversible peristaltic pump (Verderflex, Castleford, UK), controlled from the programmable logic controller (PLC) (MoreControl, Aas, Norway). A return activated sludge (RAS) line was incorporated into the system between chambers III and II, and was controlled by RAS pumping intervals: With lower RAS intervals, more sludge is returned.

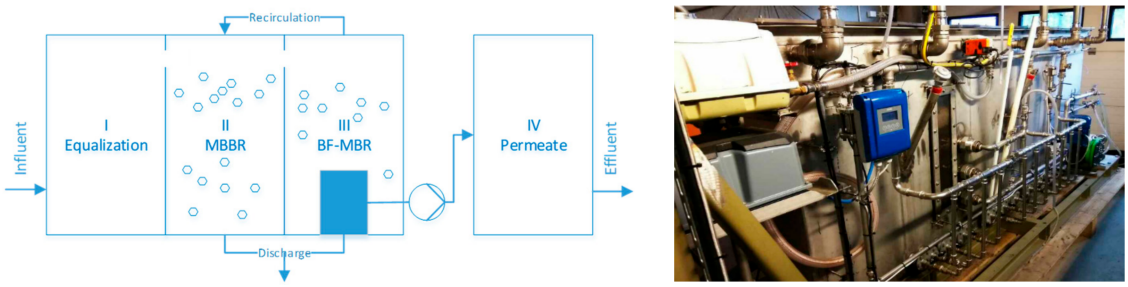

Figure 1. The BF-MBR pilot plant: Schematic diagram (**left**) and the photo of installation (**right**).

Wastewater was supplied at 0.3 m^3/day through the screens to the equalization tank (I) from the source-separated sewer network, keeping the ratio of black to grey water at 1:9. Black water was collected from the toilets and grey water from all other discharge points of the households around the pilot site [102]. This allowed maintenance of the influent quality at 1–1.3 g/L by suspended solids and 100–350 mg-O_2/L by COD.

Flat sheet SiC microfiltration membranes with 0.1 µm pore size (Cembrane, Lynge, Denmark) were used in the separation chamber (III), providing total filtering area of 0.828 m^2. Aeration was organized in chambers II and III by a MEDO LA-60E air compressor at 60 L/min.

Initial biological activity in the system was provided by inoculation with sludge from the municipal MBBR wastewater treatment plant (BEVAS, Oslo, Norway).

The BF-MBR pilot plant was operated in automatic mode under constant flux conditions, controlled through the PLC. The initial filtration settings were: 300 s of filtration at net-flux 8.2 LMH, 60 s relaxation, 15 s backwash with permeate at net-flux 180 LMH, 120 s relaxation. Further changes were introduced into the plant operation settings in order to reach different operation states (Table 2), which divided full operation time of 114 days into 8 relevant periods.

Plant operation data was continuously recorded every 3 s to the data-logger, in-built in the PLC. Values of system inflow, level in the separation chamber, TMP and permeate flow were stored and recalculated further to analytical values.

Filtration settings were programmed as $t_{filtr/relax/BW}$, filtration/relaxation/backwash time, and $RAS_{pulse\ interval}$ = RAS_{PI}, the pulse interval of the return activated sludge. For every period of operation, normalized net membrane flux was calculated ($J_{n(net)}$). The normalized permeability, P_n, and permeability slope, dP_n/dt, were determined.

Permeate flow was used to calculate membrane flux J (LMH; Equation (1)), normalized to 20 °C as J_n (Equation (2)), and used to calculate normalized permeability, P_n (Equation (3)), and the fouling rate in terms of membrane permeability decrease, dP_n/dt (Equation (4)):

$$J = \frac{F}{S_f} \quad (1)$$

$$J_n = J \cdot e^{(-0.032 \cdot (t-20))} \quad (2)$$

$$P_n = \frac{J_n}{TMP} \quad (3)$$

$$\frac{dP_n}{dt} = \frac{P_{ni} - P_{ni-1}}{t_i - t_{i-1}} \quad (4)$$

where F is permeate flow, L/h, and S_f is the active filtration surface (m^2).

Table 2. BF-MBR pilot plant operation settings.

Period	Days	Adjustments in Settings	Processes and Changes in the System
I	1–20	$J_{n(net)}$ [1] = 8.2 LMH, $J_{n(gross)}$ [2] = 37.6 LMH Filtration cycle settings: t_{filtr} = 300 s, t_{relaxI} = 60 s, $t_{relaxII}$ = 120 s, t_{BW} = 15 s $RAS_{pulse\ interval}$ [3] = 1620 s, SRT_{av} [4] =20 days	Conditions for sludge adaptation and conditional fouling of fresh membranes.
II	21–34	$J_{n(net)}$ [1] = 5.3 LMH, $J_{n(gross)}$ [2] = 32.6 LMH, $RAS_{pulse\ interval}$ [3] = 740 s, SRT_{av} [4] =20 days	System stabilization and an increase of sludge recirculation between separation and MBBR [5] chambers through the decrease of RAS [6] interval.
III	35–36	$J_{n(net)}$ [1] = 12.2 LMH, $J_{n(gross)}$ [2] = 44.0 LMH	Increase of net-flux in order to get close to TMP [7] jump.
IV	37–44	$J_{n(net)}$ [1] = 10.0 LMH, $J_{n(gross)}$ [2] = 43.7 LMH, t_{BW} = 19.5, t_{relaxI} = 30	Prolongation of backwash in order to stabilize the system and TMP [7] jump.
V	45–47	CIP [8] I, 1% NaOCl, 2% Citric acid	TMP [7] ↓; P_n ↑ (58%), dP_n/dt ↑ (88%)—removal of reversible and irreversible fouling.
VI	48–77	Same as in period IV, SRT = 31 days	Reproduction of last stable operation.
VII	78–85	CIP [8] II	TMP [7] ↓ (82%), P_n ↑ (82%), dP_n/dt ↑.
VIII	86–114	$J_{n(net)}$ [1] = 4.5 LMH, $J_{n(gross)}$ [2] = 30.4 LMH, Infinite SRT (no wastage/sludge discharge)	Lower hydraulic loading.

Notes: [1] Normalized net flux; [2] Normalized gross flux; [3] The pulse interval of the return activated sludge; [4] Average solids retention time; [5] Moving-bed-biofilm reactor; [6] Return activated sludge; [7] Transmembrane pressure; [8] Cleaning-in-place.

The data array of hydraulic parameters was statistically treated and expressed in the form of 8 representative filtration cycles for every day. For a single cycle, a set of average initial (TMP_i, J_{Ni}, P_{ni}) and final parameters (TMP_{i-1}, J_{Ni-1}, P_{ni-1}) was calculated, excluding ramp and relaxation periods of the peristaltic pump.

Recovery of membrane permeability was expressed as the ratio of permeability after chemical cleaning and before chemical cleaning [103]:

$$Recovery_{P_n} = \frac{P_{CIP/BW_{fin}} - P_{CIP/BW_{in}}}{P_{in} - P_{fin}} \quad (5)$$

where: $P_{CIP/BW_{fin}}$ is a permeability of the new filtration cycle after the backwash/Chemical cleaning (CIP); $P_{CIP/BW_{in}}$ is the initial permeability before the cleaning, which is equal to P_{fin}, the permeability at the end of previous filtration cycle; and, P_{in} is the initial permeability at the beginning of the previous filtration cycle.

In other words, recovery of permeability expresses the extent to which membrane permeability is restored after the application of different types of cleaning to remove the foulants [104].

A sampling of mixed liquor, and raw and treated wastewater was organized on a daily basis. Samples of raw wastewater (chamber I), MBBR mixed liquor (chamber II), BF-MBR mixed liquor (chamber III) and permeate (chamber IV) were analyzed accordingly for suspended solids (SS, MLSS), COD of the filtrates, DSVI, and RH. COD was measured by COD-cuvette test (HACH, Manchester, UK)

applying the dichromate method, DSVI was measured by a settleability test. RH was determined by the MATH (microbial adherence to hydrocarbons) method. The analyses were conducted in accordance with SMWW (Standard Methods for the Examination of Water and Wastewater) (22nd edition) and the MATH test [59,105]. Flow in permeate line and TMP were measured through flow and pressure sensors (Krohne, Dilling, Norway) and logged every second to the PLC together with filtration cycle settings.

PLS regression was used to distinguish the relationship between the parameters of the mixed liquor and the fouling indicators and to predict the fouling intensity. The statistical software, The Unscrambler® X10.3 (CAMO Software AS, Oslo, Norway), was used to perform the analysis of the monitored data.

3. Results and Discussion

3.1. Pilot Plant Operation Results

During 114 days of operation of the BF-MBR pilot plant, notable trends in TMP, permeability, permeability slope, MLSS in the membrane separation chamber (MLSS-III) and COD removal were observed (Figure 2), allowing the development of the qualitative description of the biological activity and its influence on membrane separation process.

The first period (1–20 days) can be described as the period of biological adaptation and biomass development. It is characterized by moderate growth of biomass up to MLSS-III 5–6 g/L and increasing biodegradation of organics in the range of 67–81%, together with a steep TMP growth and a respective decrease of permeability at a relatively high rate of 0.35–0.47 LMH/bar/s. This state can be identified as conditioning fouling.

After reaching the conditionally critical value of 1.7 times permeability decrease, the return of suspended solids from separation chamber (III) to MBBR chamber (II) was doubled, leading to stabilization of permeability and MLSS-III in the next period (21–34 days) and decreasing the membrane fouling rate to 0.25–0.27 LMH/bar/s by permeability, which is considered steady fouling.

In order to increase the system productivity in terms of permeate, membrane flux was increased, entailing the TMP jump during the third period (35–36 days), which indicates a severe fouling. Following that, backwash and relaxation times were adjusted in order to stabilize rapid fouling development during 37–44 days.

Chemical cleaning (CIP), applied in the fifth period, exhibited relatively high values of the recovered membrane permeability. While recovery of the permeability between the backwashes performed at the end of every filtration cycle was in the range 88–126%, recovery of the permeability after CIP was in the range of 158–182%.

The sixth period (48–77 days) was another steady fouling state. It reproduced the same trends from the second period (21–34 days), except for a more stable COD degradation due to well-developed biofilms in MBBR part and on carriers in the separation chamber (III). After reaching 400 mbar of TMP, a second chemical cleaning was provided, applying higher backwash pressure with the subsequent soaking of the membrane elements in the cleaning solutions, which caused the permeability to recover to the initial value.

The last, eighth period of system operation is a control period which is characterized by both conditional and steady fouling in the permeability pattern.

In general, in the way described above, the operation of the BF-MBR pilot plant was observed during all the states, which is important for the determination of membrane fouling patterns: Conditional fouling, steady fouling, and TMP jump at different fluxes. Two chemical cleaning procedures were conducted to estimate the recovery of permeability. Data, which were recorded during these states, were taken as the basis for further statistical analysis.

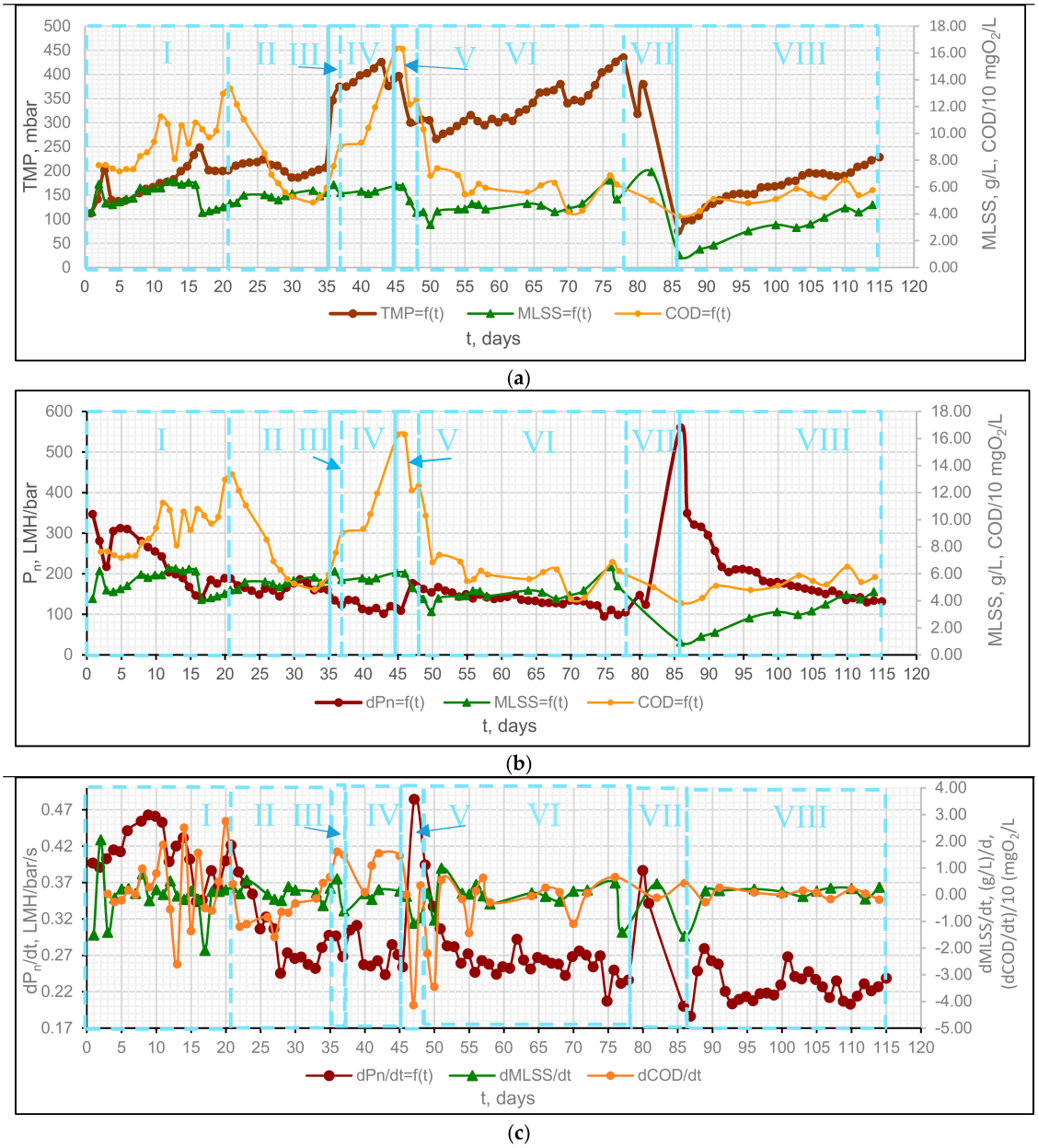

Figure 2. BF-MBR pilot plant operation profile: (**a**) TMP, MLSS-III, COD-III change within operation time; (**b**) normalized permeability (P_n), MLSS-III, COD-III change within operation time; (**c**) first derivative of normalized permeability (dP_n/dt), MLSS-III (dMLSS/dt), COD-III (dCOD/dt) within operation time.

3.2. Statistical Determination of Membrane Fouling Patterns

According to the literature, the influence of the mixed liquor parameters (i.e., MLSS, SVI (DSVI), COD, and RH) on the filtration performance and fouling intensity is controversial. Indeed, a positive impact of higher MLSS concentration on MBR hydraulic performance has been indicated [15,106]. On the contrary, Chang et al. [46] observed a positive link between the MLSS increase and the flux decline, which is the opposite of its effect on the specific cake resistance, while Brookes et al. [107] and Jefferson et al. [108] showed that MLSS concentration is not a governing factor influencing the overall membrane fouling, and no consistent correlation was observed between MLSS and fouling intensity.

The influence of the relative hydrophobicity on system performance is also not fully comprehended. According to the findings by Deng et al. [40] and Huang et al. [109], high RH fosters the mitigation of fouling due to the weaker interactions of hydrophobic flocs with a hydrophilic membrane. In addition, lower RH values entail floc deterioration and the consequent increase of cake layer resistance [29], whereas higher RH values are associated with better flocculation [60]. Meanwhile, as specified by Meng et al. [36] and Tian et al. [64], higher RH of sludge causes the formation of a more dense cake layer on the membrane surface, resulting in a greater TMP rise.

There is a lack of data on the correlation between SVI and membrane fouling intensity. Chae et al. [110] stated that high SVI values corresponded to severe membrane fouling in an MBR system. Ng et al. [111] linked the increased SVI values to the higher ratio of non-flocculating components of the activated sludge but did not mention if this affected the fouling intensity. In contrast, according to Fan et al. [112] and Wu and Huang [113], this parameter is not a reliable indicator to predict the membrane fouling potential for MBR systems and has no effect on membrane filterability.

As found, COD is indirectly related to the fouling intensity. COD is linked to the concentration of soluble foulants which have a negative effect on membrane filterability [114]. In addition, COD in the effluent from aerobic and anaerobic biological systems is encountered in the form of soluble microbial products which are among the foulants in MBRs [115]. Meanwhile, Lesjean et al. [116] found no clear correlation between COD and the fouling intensity.

Hence, to gain a deeper understanding of the role of the mixed liquor characteristics in the filtration performance of the investigated system, it was decided to monitor these parameters and their variation over time in the separation chamber (Table 3) and to process the collected data statistically.

Table 3. Parameters of the mixed liquor in the separation chamber.

Parameter	Value
MLSS, g/L	5–6.5
dMLSS/dt, (g/L)/day	−0.61–2.06
DSVI, mL/g	118–272
dDSVI/dt, (mL/g)/day	−91–57
RH, %	20.5–61.5
dRH/dt, %/day	−27–35
COD_{dis}, mgO_2/L	38–134
dCOD/dt, mgO_2/L/day	−35–27.5

Since the operating conditions varied significantly throughout the whole filtration period (Table 2), which influenced both the activated sludge parameters and the fouling indicators, it was decided to split the whole data range into its characteristic phases and statistically analyze them separately from each other, excluding the data which covered the chemical cleanings. Hence, three basic periods were established: period A (days 3–34), period B (days 49–77) and period C (days 86–114).

PLS regression (also known as a projection of latent structures) was used as an advanced mathematical and statistical tool to model the relations between the X variables and the Y responses within every single period (Table 4).

Table 4. Model inputs.

Period	Predictors	Responses
A	MLSS, dMLSS/dt, DSVI dDSVI/dt, RH, dRH/dt, COD_{dis}, dCOD/dt	TMP, P_n, dP_n/dt
B	MLSS, dMLSS/dt, DSVI dDSVI/dt, COD_{dis}, dCOD/dt	TMP, P_n, dP_n/dt
C	MLSS, dMLSS/dt, DSVI dDSVI/dt, COD_{dis}, dCOD/dt	TMP, P_n, dP_n/dt

The X- and Y-matrices were modelled simultaneously to find the latent variables in input X parameters that best predicted the latent variables in the corresponding Y responses (i.e., PCAs on the

X- and Y-data were performed with the subsequent acquisition of the relative scores). Then, the plotting of two sets of the scores (those related to X and Y) against each other was conducted, maximizing the covariance between X and Y [117].

The obtained model was validated by applying a random cross-validation in PLS. The number of PLS components (factors), was chosen according to the explained variance.

The results of the performed analyses of the data from the initial period of the system performance (Period A) are shown below (Figure 3).

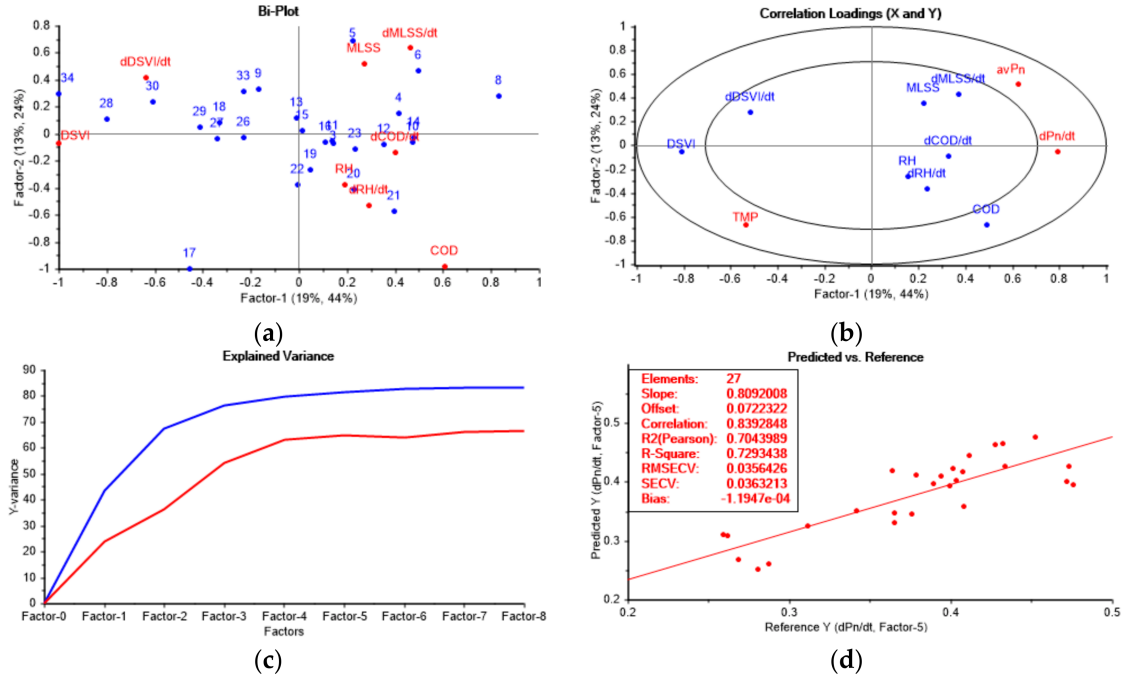

Figure 3. Results of PLS of the data from the period A of the filtration performance monitoring: (**a**) Bi-plot; (**b**) loadings plot; (**c**) explained variance plot; (**d**) fouling intensity prediction model.

The correlation loadings plot is computed by accounting for each variable for the displayed latent variables (factors). From the loadings plot, Factor-1 clearly describes DSVI, dDSVI/dt, TMP, COD, dMLSS/dt, permeability, P_n, and its slope, dP_n/dt, since the first three variables are located at the far left, and the rest at the far right along the Factor-1 axis. Factor-1 also accounts for dCOD/dt, while MLSS and dRH/dt mainly contribute to Factor-2. According to the PLS loadings plot, COD and DSVI explain more than 50% of the variance and are probably the most important variables. DSVI has a negative correlation with both permeability and permeability slope, but is positively linked to TMP. Particularly in this case, COD has a negative correlation with the variables DSVI, dDSVI/dt, MLSS and dMLSS/dt, and is negatively linked to the average normalized permeability (nP). Although the rest of the variables are located in the inner ellipse, which indicates up to 50% of the explained variance and thus does not contain enough structured variation to discriminate between the mixed liquor samples, it was decided to keep them to make the model more reliable.

The analysis of the scores and loadings plot and the bi-plot demonstrates that the samples from days 1–20 are mostly characterized by higher RH, dRH/dt, MLSS, dMLSS/dt, COD, and dCOD/dt, while the samples taken during the period 22–34 day have higher DSVI and dDSVI/dt values.

As demonstrated by the graph of explained variance (Figure 3c), it is preferable to use five components, since this number gives a lower residual variance.

According to the Figure 3d (the validation graph), the developed model is linear (R-squared = 0.73) and with a reasonable fit to the majority of data: Slope = 0.81, offset 0.07 and the dispersion of the validation samples around the regression line (Root Mean Square Error of Cross Validation–RMSEV)

and the standard error of cross-validation (SECV) are approximately 0.036. Consequently, the model is reliable and can be used for future predictions for the defined number of factors under the operational conditions applied during the period A.

Relative hydrophobicity and its change required much more effort and time to be experimentally determined than other variables. In addition, RH and dRH/dt are characterized by relatively low-weighted regression coefficients: 0.02 and −0.086, respectively (Factor-2); and, 0.07 and 0.04, respectively (Factor-1) (i.e., these variables are not well explained by the components). Considering the above-mentioned aspects, it was decided to exclude RH and dRH/dt from further monitoring and analysis.

The second period, B, covers the filtration performance data collected between the first and the second chemical cleanings of the system. Obtained results of the PLS analysis are represented below (Figure 4).

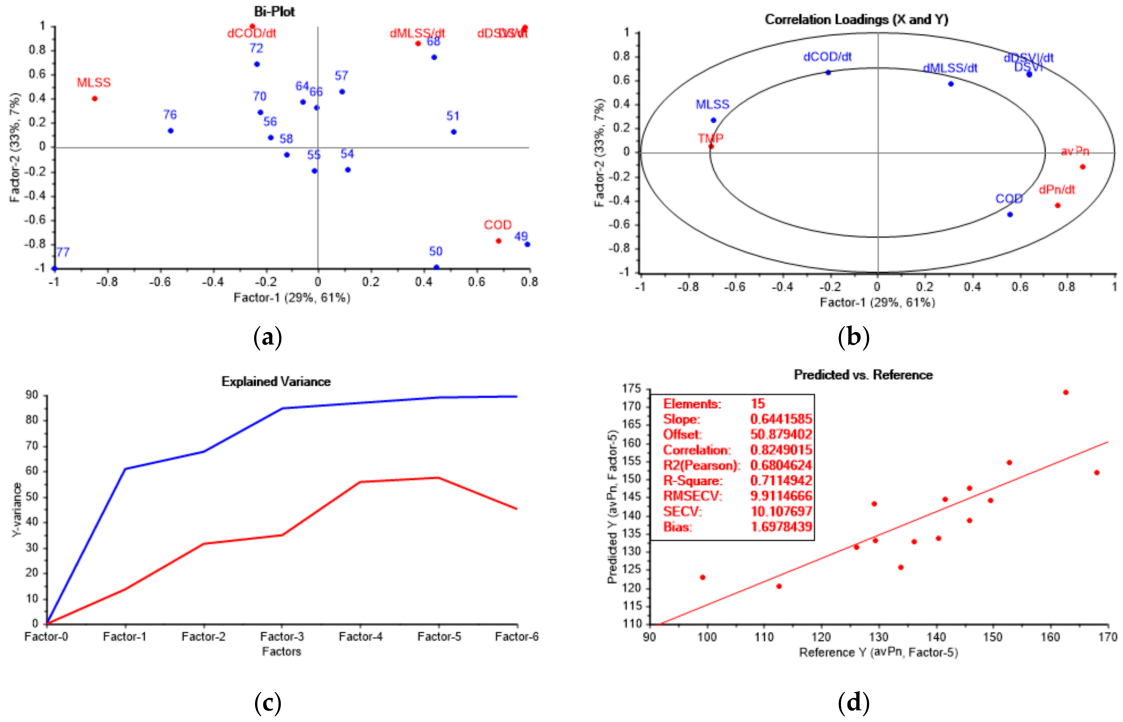

Figure 4. Results of PLS of the data from the period B of the filtration performance monitoring: (**a**) Bi-plot; (**b**) loadings plot; (**c**) explained variance plot; (**d**) fouling intensity prediction model.

According to the bi-plot (Figure 4b), the majority of the samples within period B are characterized by higher dCOD/dt values. Meanwhile, the samples taken on days 49–50 are characterized by higher COD values; on days 51, 57 and 68 by relatively high dMLSS/dt, DSVI, and dDSVI/dt values; on day 72 by comparatively high dCOD/dt values; and on days 76 and 77 by more significant MLSS values.

According to the correlation loadings plot, Factor-1 apparently describes TMP, MLSS, COD, average permeability (avP_n), dP_n/dt, DSVI and dDSVI/dt. Factor-2 is related to dCOD/dt and dMLSS/dt. All the variables were marked as significant according to the plot of correlation loadings, even though the MLSS variable gives slightly less than 50% of the explained variance. MLSS and dCOD/dt are positively linked to the TMP response, in contrast to dMLSS/dt, DSVI, dDSVI/dt, which have a negative correlation with TMP and the permeability slope (dP_n/dt). The COD variable has a high positive correlation with dP_n/dt and is positively linked to the average permeability (avP_n).

Figure 4 demonstrates that the optimum number of factors is five, which provides more than 57% of the explained Y-variance.

An analysis of the validation plot shows that the developed model is linear, having R-squared = 0.71 and with a good fit to the majority of data (i.e., slope = 0.64). RMSEV and SECV are approximately 10, but it is essential to acknowledge that the mentioned errors have the same units as the reference Y (in this case, average normalized permeability, avP_n). R-squared (Pearson) is close to R-squared correlation (0.68 vs. 0.82), which indicates the reliability of the model. Consequently, a good prediction is attained with the developed model, which proves that the model is reliable and can be used during further stages when the operating conditions applied in the period B are replicated.

The output from the PLS modelling of the data acquired after the second CIP (the period C) is demonstrated below (Figure 5).

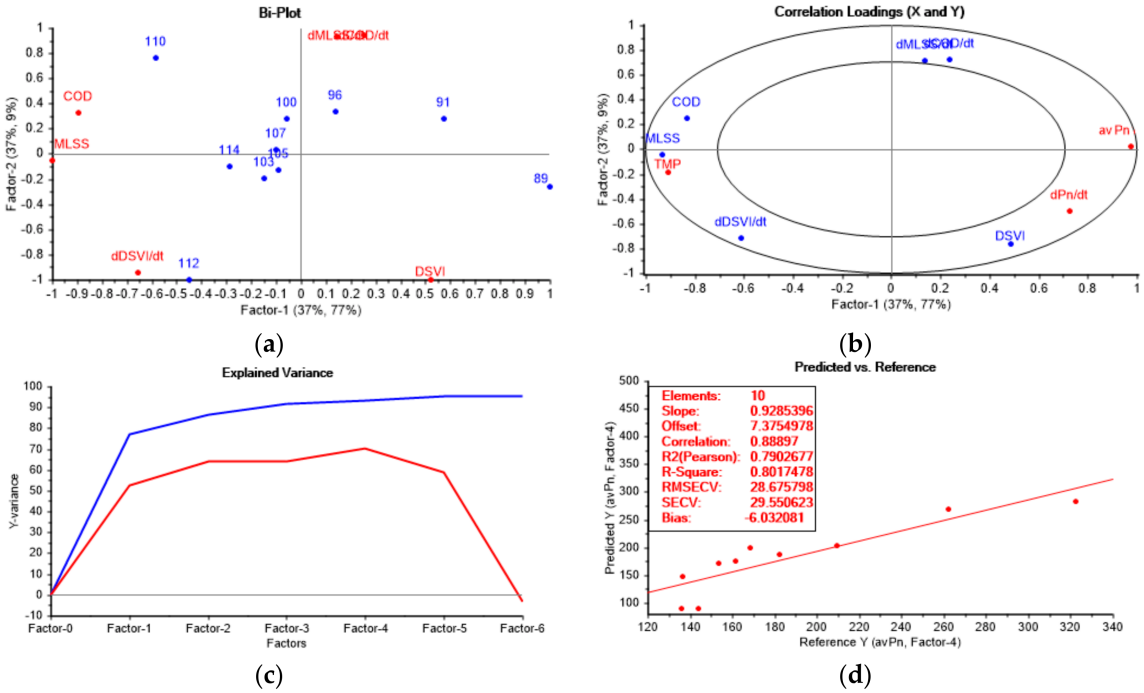

Figure 5. Results of PLS of the data from the period C of the filtration performance monitoring: (**a**) Bi-plot; (**b**) loadings plot; (**c**) explained variance plot; (**d**) fouling intensity prediction model.

The bi-plot shows that the samples from day 89 have a higher DSVI value, while dMLSS/dt and dCOD/dt are the most distinctive parameters for days 91 and 96. Days 100, 107 and 110 are characterized by higher COD content, whereas days 103, 105 and 114 have higher MLSS values. Day 112 is characterized by a higher dDSVI/dt.

From the correlation loadings plot (Figure 5b), COD, MLSS, TMP, dDSVI/dt, DSVI, avP_n and dP_n/dt contribute to Factor-1, while Factor-2 describes dMLSS/dt and dCOD/dt. All the specified variables explain more than 50% of the variance and thus have high importance in relation to Factor-1 and Factor-2. MLSS and dDSVI/dt are positively linked to TMP and have a negative correlation with the permeability indicators, avP_n and dP_n/dt. DSVI is positively correlated to dP_n/dt, while dMLSS/dt and dCOD/dt have a negative correlation with the permeability slope.

The explained variance plot indicates that the optimum number of factors is four, which provides more than 70% of explained Y-variance.

The points of the validation graph in Figure 5d have a linear trend (R-squared = 0.8), having a good fit to the majority of data (slope = 0.93). R-squared (Pearson) is close to R-squared correlation (0.79 vs. 0.89), which indicates the reliability of the model. Only the errors RMSEV and SECV are higher than in previous cases, but this can be explained by the higher values of the response function (average permeability) in this particular case.

Since the higher amount of data was available to be collected during the last period C (Table 5) in comparison to the previous modes, it was decided to apply the predict function to new data.

Table 5. Mixed liquor characteristics and fouling indicators during period VIII (new data).

	TMP_{av} [1], Bar	av dP_n/dt [2]	avP_n [3], LMH/Bar	DSVI [4], mL/g	dDSVI/dt [5]	MLSS [6], g/L	dMLSS/dt [7]	COD_f [8], mgO_2/L	dCOD/dt [9]
max.	266.16	0.26	125.45	185.41	5.52	5.74	0.35	69.80	5.00
min.	232.30	0.23	112.98	142.60	−7.79	5.32	−0.17	45.40	−3.83
average	249.26	0.24	120.66	166.56	−1.96	5.48	0.02	55.52	−0.44

Notes: [1] Average transmembrane pressure; [2] Average normalized permeability slope; [3] Average normalized permeability; [4] Diluted sludge volume index; [5] Diluted sludge volume index slope; [6] Mixed liquor suspended solids; [7] Mixed liquor suspended solids slope; [8] Chemical oxygen demand (filtered); [9] Chemical oxygen demand slope.

Full prediction with the identification of outliers was used. The following results were obtained (Figure 6).

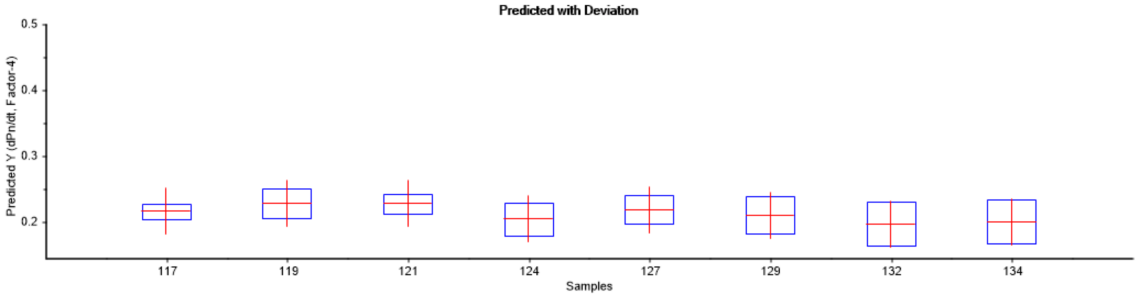

Predicted Y	Predicted	Deviation	Reference
117	0.2146	0.0113	0.2349
119	0.2265	0.0222	0.2453
121	0.2262	0.0156	0.2538
124	0.2029	0.0251	0.2327
127	0.2175	0.0218	0.2396
129	0.2092	0.0280	0.2510
132	0.1954	0.0334	0.2358
134	0.1994	0.0340	0.2590

Figure 6. Prediction results for the new data from Period C for four factors using the derived PLS model for the relevant period.

The deviation between the predicted and the reference values is in the range 0.01–0.034, which demonstrates the reliability of the applied model.

Consequently, a good prediction is attained by applying the developed model, which proves that the model is reliable and can be used during further stages under the operating conditions that were applied during period C.

In addition, MLR was performed using leverage correction. However, obtained results are unreliable since the same data was validated and used for the prediction, which provided overly optimistic results. The application of the test matrix in MLR would merely copy the PLS strategy but do so in a more difficult way. MLR is a simpler way of doing the calculations, but PLS is much more advanced due to the applied validation techniques.

SRT and permeate flux are among the key operating parameters controlling fouling intensity in MBR.

In order to estimate the influence of SRT on the performance of the current system, this parameter was included in the models as an additional variable. The acquired results are represented in Figure 7.

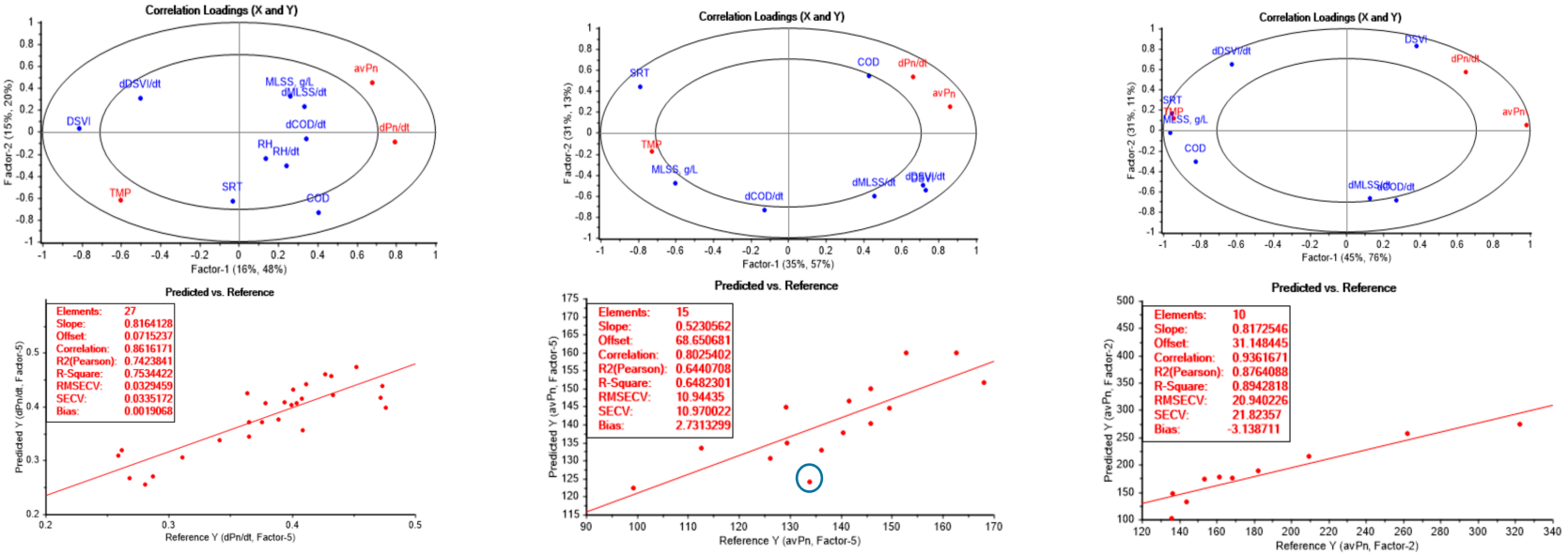

Figure 7. Results of PLSs of the data from all the periods of the filtration performance monitoring, including SRT: (**a**) period A; (**b**) period B; (**c**) period C.

According to the correlation loadings plot related to period A, SRT explains less than 50% of the variance and thus has relatively little influence. In this particular case, SRT exhibits an independent variation in relation to other variables, except for COD, which has a weak positive link with SRT. Meanwhile, SRT exhibits a slightly negative correlation with the normalized permeability and permeability slope for period A. Concerning the model enhancement, the introduction of the new variable did not entail any significant improvement: RMSECV was just 0.002 less than its value in the initial model, while the bias, on the contrary, showed an order of magnitude increase in absolute value.

The results related to period B demonstrate that SRT is an important variable which explains more than 50% of the variance in the dataset. It has a strong negative correlation with COD and the normalized permeability. In addition, SRT is positively correlated with MLSS along Factor-1. The negative correlation between SRT and COD during this period can be attributed to the higher treatment performance of the biomass, which becomes well-developed at SRT up to 40 days and thus is capable of a more efficient biodegradation of organic contaminants, particularly SMPs, causing the decrease of COD values [118,119]. Meanwhile, the increase in SRT promotes the development of higher MLSS concentrations [120], thus inducing membrane fouling.

The introduction of the new variable into the existing model decreased its linearity R-squared = 0.65 vs. R-squared = 0.71 (values in the new model vs. values characteristic for the basic model related to period B), with a slightly worse fit to the majority of data (slope = 0.52 vs. slope = 0.64), RMSEV 10.9 vs. 9.9, SECV 10.97 vs. 10.1, bias 2.73 vs. 1.7. In addition, the new model underestimated a sample from day 72 (marked with the blue circle).

The modelling of the dataset from period C demonstrates the importance of the SRT variable. SRT is highly positively correlated with MLSS and TMP, and is negatively linked to normalized permeability and its slope, hence indicating the fouling enhancement through the increase of MLSS at higher SRTs, which agrees with the previous findings by Le-Clech et al. [29], Van den Broeck et al. [120], Yigit et al. [121]. The positive link between SRT and COD along Factor-1 during this period can be attributed to the accumulation of small microbial by-products (SMP with the molecular weight (MW) < 1 kDa), which contribute to fouling through deflocculation at high SRTs (>31 days) [118,121,122]. However, further studies are required to confirm the presence of different groups of microorganisms at various SRTs in this system (for example, tightly and loosely bound EPS, small SMP, etc.), since the deep investigation of the biomass content was not in the scope of the current research.

The new model exhibits higher linearity (R-squared = 0.89 vs. R-squared = 0.80) and a slightly higher accuracy (RMSEV = 20.9 vs. RMSEV = 28.7; SECV = 21.8 vs. SECV = 29.6; and, bias = −3.4 vs. bias = −6.0) than the initial model.

It is noteworthy that the purpose of including SRT in modelling was not to improve the models for the relevant periods developed earlier in this work, since the inclusion of a new variable is undesirable as it could complicate the model (i.e., it is preferable to use as low a number of variables as possible) [123]. Besides, the introduction of the SRT variable to the model covering period C barely decreased the deviation in the prediction of the new dataset (Table 4; 0.016–0.0261 vs. 0.011–0.034), making the extension of the model size unreasonable for its further use in the system controller. The scope was to show the influence of SRT on the operational parameters and fouling intensity in the current system to achieve the highest possible fouling inhibition.

As discovered, SRT should be less than 31 days to avoid a severe membrane fouling. This can be called the critical SRT. The SRT that can be applied without a sharp decrease in permeability is 20 days for the current BF-MBR system. In the studied pilot plant, SRT was adjusted by changing the frequency of sludge removal and the volume of the removed sludge per batch.

Concerning the permeate flux, it can be decreased in order to minimize the filtration resistance if the biomass exhibits high fouling propensity. The current system worked at a constant permeate flux, which varied depending on the monitoring period (Table 2). In general, all the applied fluxes were below the critical flux value to avoid a severe membrane fouling [124–126]. The critical net flux was determined by the flux-step method, described by Miller et al. [127], and was in a range of 12–15 LMH.

In addition to the desludging option, the concentration of the mixed liquor in the separation and biological chambers was regulated by adjusting the RAS pumping intensity (i.e., pulse length and frequency). The introduction of the RAS line made it possible to build up the desired level of biomass in biological and separation chambers, and to adjust the endogenous decay of the biomass, thus providing sufficient COD and NH_4^+ removal.

To summarize, the monitored mixed liquor characteristics allowed the controlling of the fouling intensity by adjusting the operating conditions which helped to maintain the stability of the system performance and, hence, the permeate quality: BF-MBR installation assured 100% MLSS elimination and 67–90% treatment efficiency in terms of COD removal, keeping the TMP below 500 mbar.

4. Conclusions

The developed chemometric approach to the assessment of membrane fouling in membrane bioreactor advances the field of fouling monitoring and provides a statistical tool for its control in submerged membrane bioreactors.

The approach was based on PLS regression analysis and was used to detect membrane fouling patterns in the biofilm ceramic membrane bioreactor pilot system during 114 days of operation, varying membrane flux and solid retention time, and covering the periods of steady fouling and TMP jumps, followed by two chemical cleanings in the system.

The mixed liquor parameters MLSS, dMLSS/dt, DSVI, dDSVI/dt, COD, and dCOD/dt were found to be significant for estimation and prediction of fouling intensity, while relative hydrophobicity of mixed liquor and its slope seemed to play a secondary role. Normalized permeability and its slope were identified as the most reliable fouling indicators, while critical solid retention time was introduced as another quantitative parameter, influencing the intensity of membrane fouling.

The cross-validation of every model and the complete validation of the model, covering the last phase of the filtration, demonstrated low uncertainty of the predictions, and hence high reliability of the models, allowing further implementation of the developed fouling control strategies.

The models were used to adjust operational parameters of the pilot system according to the characteristics of biomass, keeping the system running below critical transmembrane pressure (500 mbar), with 67–90% removal of chemical oxygen demand and 100% retention of suspended solids, resulting in good recovery of membrane permeability after chemical cleanings, thus removing irreversible fouling.

Further work is foreseen in the validation of the developed approach in an operational environment of decentralized membrane bioreactors, where the sustainable operation is frequently a critical issue due to the lack of qualified supervision, and which raises the barrier to penetration of membrane bioreactors into cost-sensitive markets.

Author Contributions: O.K. and Z.M. conceived and designed the experiments; O.K. performed the experiments under supervision of Z.M. and analyzed the data; H.R. contributed reagents, materials and analysis tools, and contributed to the discussion of the article; O.K. wrote the paper with advice from Z.M.

Funding: This research was co-funded by the Erasmus+ Program of the European Union (project number: 561755-EPP-1-2015-1-NOEPPKA2-CBHE-JP).

Acknowledgments: Authors express their gratitude to Daniel Todt from Ecomotive AS for facilitating pilot plant studies; Yuliia Dzihora and Stella Saliu for their inputs as Erasmus+ exchange students; Knut Kvaal for his guidance on mathematical modelling using the Unscrambler software.

Conflicts of Interest: The authors declare no conflict of interest. The founding sponsors had no role in the design of the study; in the collection, analyses, or interpretation of data; in the writing of the manuscript, and in the decision to publish the results.

References

1. World Economic Forum. The Global Risks Report 2018. Available online: https://www.weforum.org/reports/the-global-risks-report-2018 (accessed on 9 December 2017).

2. World Economic Forum. Grim Reaping. Available online: http://reports.weforum.org/global-risks-2018/grim-reaping/ (accessed on 10 December 2017).
3. United Nations World Water Assessment Programme (WWAP). *The United Nations World Water Development Report 2017, Wastewater: The Untapped Resource*; UNESCO: Paris, France, 2017.
4. Lautze, J.; Stander, E.; Drechsel, P.; da Silva, A.K.; Keraita, B. *Global Experiences in Water Reuse*; International Water Management Institute (IWMI): Colombo, Sri Lanka; CGIAR Research Program on Water, Land and Ecosystems (WLE): Montpellier, France, 2014; 31p.
5. European Commission. Water is too Precious to Waste. Available online: http://ec.europa.eu/environment/water/pdf/water_reuse_factsheet_en.pdf (accessed on 13 January 2018).
6. Hwang, H.; Forrester, A.; Lansey, K. Decentralized water reuse: Regional water supply system resilience benefits. *Procedia Eng.* **2014**, *70*, 853–856. [CrossRef]
7. Lesjean, B.; Leiknes, T.; Hochstrat, R.; Schories, R.; Gonzalez, G.; Gonzalez, A. MBR: Technology gets timely EU cash boost. *Filtr. Sep.* **2006**, *43*, 20–23. [CrossRef]
8. Hai, F.I.; Yamamoto, K.; Lee, C.-H. *Membrane Biological Reactors: Theory, Modeling, Design, Management and Applications to Wastewater Reuse*; IWA Publishing: London, UK, 2014; 504p, ISBN 9781780400655.
9. Geilvoet, S.P. The Delft Filtration Characterisation Method: Assessing Membrane Bioreactor Activated Sludge Filterability. Ph.D. Thesis, Delft University of Technology, Delft, The Netherlands, 12 February 2010.
10. Global $8.27 Bn Membrane Bioreactor Market, 2025. Available online: http://markets.businessinsider.com/news/stocks/global-8-27-bn-membrane-bioreactor-market-2025-1005680257 (accessed on 15 December 2017).
11. Böhm, L.; Drews, A.; Prieske, H.; Bérubé, P.R.; Kraume, M. The importance of fluid dynamics for MBR fouling mitigation. *Bioresour. Technol.* **2012**, *122*, 50–61. [CrossRef] [PubMed]
12. Ivanovic, I.; Leiknes, T.O. The biofilm membrane bioreactor (BF-MBR)—A review. *Desalination Water Treat.* **2012**, *37*, 288–295. [CrossRef]
13. Ivanovic, I.; Leiknes, T.O.; Ødegaard, H. Fouling control by reduction of submicron particles in a BF-MBR with an integrated flocculation zone in the membrane reactor. *Sep. Sci. Technol.* **2008**, *43*, 1871–1883. [CrossRef]
14. Yu, H.Y.; Xu, Z.K.; Lei, H.; Hu, M.X.; Yang, Q. Photoinduced graft polymerization of acrylamide on polypropylene microporous membranes for the improvement of antifouling characteristics in a submerged membrane-bioreactor. *Sep. Purif. Technol.* **2007**, *53*, 119–125. [CrossRef]
15. Brookes, A.; Jefferson, B.; Guglielmi, G.; Judd, S.J. Sustainable Flux Fouling in a Membrane Bioreactor: Impact of Flux and MLSS. *Sep. Sci. Technol.* **2006**, *41*, 1279–1291. [CrossRef]
16. Kraume, M.; Wedi, D.; Schaller, J.; Iversen, V.; Drews, A. Fouling in MBR: What use are lab investigations for full scale operation? *Desalination* **2009**, *236*, 94–103. [CrossRef]
17. Yusuf, Z.; Wahab, N.A.; Abusam, A. Neural Network-based Model Predictive Control with CPSOGSA for SMBR Filtration. *Int. J. Electr. Comput. Eng.* **2017**, *7*, 1538–1545. [CrossRef]
18. Song, W.; Li, Z.; Li, Y.; You, H.; Qi, P.; Liu, F.; Loy, D.A. Facile sol-gel coating process for anti-biofouling modification of poly (vinylidene fluoride) microfiltration membrane based on novel zwitterionic organosilica. *J. Membr. Sci.* **2018**, *550*, 266–277. [CrossRef]
19. Gkotsis, P.K.; Mitrakas, M.M.; Tolkou, A.K.; Zouboulis, A.I. Batch and continuous dosing of conventional and composite coagulation agents for fouling control in a pilot-scale MBR. *Chem. Eng. J.* **2016**, *311*, 255–264. [CrossRef]
20. Lee, J.C.; Kim, J.S.; Kang, I.J.; Cho, M.H.; Park, P.K.; Lee, C.H. Potential and limitations of alum or zeolite addition to improve the performance of a submerged membrane bioreactor. *Water Sci. Technol.* **2001**, *43*, 59–66. [CrossRef] [PubMed]
21. Zarei, A.; Moslemi, M.; Mirzaei, H. The Combination of KMnO4 Oxidation and Polymeric Flocculation for the Mitigation of Membrane Fouling in a Membrane Bioreactor. *Sep. Purif. Technol.* **2016**, *159*, 124–134. [CrossRef]
22. Drews, A. Membrane fouling in membrane bioreactors—Characterisation, contradictions, cause and cures. *J. Membr. Sci.* **2010**, *363*, 1–28. [CrossRef]
23. Zheng, Y.; Zhang, W.; Tang, B.; Ding, J.; Zheng, Y.; Zhang, Z. Membrane fouling mechanism of biofilm-membrane bioreactor (BF-MBR): Pore blocking model and membrane cleaning. *Bioresour. Technol.* **2018**, *250*, 398–405. [CrossRef] [PubMed]

24. Leiknes, T.; Ødegaard, H. The development of a biofilm membrane bioreactor. *Desalination* **2007**, *202*, 135–143. [CrossRef]
25. Jin, L.; Ong, S.L.; Ng, H.Y. Fouling control mechanism by suspended biofilm carriers addition in submerged ceramic membrane bioreactors. *J. Membr. Sci.* **2013**, *427*, 250–258. [CrossRef]
26. Arabi, S.; Nakhla, G. Impact of cation concentrations on fouling in membrane bioreactors. *J. Membr. Sci.* **2009**, *343*, 110–118. [CrossRef]
27. Chang, I.S.; Judd, S.J. Domestic wastewater treatment by a submerged MBR (membrane bio-reactor) with enhanced air sparging. *Water Sci. Technol.* **2003**, *47*, 149–154. [CrossRef] [PubMed]
28. Judd, S. *The MBR Book Principles and Applications of Membrane Bioreactors in Water and Wastewater Treatment*, 1st ed.; Elsevier Ltd.: London, UK, 2006; p. 325, ISBN-13 978-1-85-617481-7.
29. Le-Clech, P.; Chen, V.; Fane, T.A.G. Fouling in membrane bioreactors used in wastewater treatment. *J. Membr. Sci.* **2006**, *284*, 17–53. [CrossRef]
30. Mafirad, S.; Mehrnia, M.R.; Azami, H.; Sarrafzadeh, M.H. Effects of biofilm formation on membrane performance in submerged membrane bioreactors. *Biofouling* **2011**, *27*, 477–485. [CrossRef] [PubMed]
31. Meng, F.; Zhang, S.; Oh, Y.; Zhou, Z.; Shin, H.-S.; Chae, S.-R. Fouling in membrane bioreactors: An updated review. *Water Res.* **2017**, *114*, 151–180. [CrossRef] [PubMed]
32. Fallis, A. Experimental Methods in Wastewater Treatment. *J. Chem. Inf. Model.* **2013**, *53*. [CrossRef]
33. Ferreira, M.L. Filterability and Sludge Concentration in Membrane Bioreactors. Ph.D. Thesis, Delft University of Technology, Delft, The Netherlands, 15 September 2011.
34. Meng, F.; Shi, B.; Yang, F.; Zhang, H. Effect of hydraulic retention time on membrane fouling and biomass characteristics in submerged membrane bioreactors. *Bioprocess Biosyst. Eng.* **2007**, *30*, 359–367. [CrossRef] [PubMed]
35. Ji, L.; Zhou, J. Influence of aeration on microbial polymers and membrane fouling in submerged membrane bioreactors. *J. Membr. Sci.* **2006**, *276*, 168–177. [CrossRef]
36. Meng, F.; Zhang, H.; Yang, F.; Zhang, S.; Li, Y.; Zhang, X. Identification of activated sludge properties affecting membrane fouling in submerged membrane bioreactors. *Sep. Purif. Technol.* **2006**, *51*, 95–103. [CrossRef]
37. Vanysacker, L.; Boerjan, B.; Declerck, P.; Vankelecom, I.F.J. Biofouling ecology as a means to better understand membrane biofouling. *Appl. Microbiol. Biotechnol.* **2014**, *98*, 8047–8072. [CrossRef] [PubMed]
38. Wu, B.; Fane, A.G. Microbial relevant fouling in membrane bioreactors: Influencing factors, characterization, and fouling control. *Membranes* **2012**, *2*, 565–584. [CrossRef] [PubMed]
39. Zhou, Z.; Meng, F.; He, X.; Chae, S.-R.; An, Y.; Jia, X. Metaproteomic analysis of biocake proteins to understand membrane fouling in a submerged membrane bioreactor. *Environ. Sci. Technol.* **2015**, *49*, 1068–1077. [CrossRef] [PubMed]
40. Deng, L.; Guo, W.; Hao, H.; Farzana, M.; Zuthi, R.; Zhang, J.; Liang, S.; Li, J.; Wang, J.; Zhang, X. Membrane fouling reduction and improvement of sludge characteristics by bioflocculant addition in submerged membrane bioreactor. *Sep. Purif. Technol.* **2015**, *156*, 450–458. [CrossRef]
41. Lee, W.; Kang, S.; Shin, H. Sludge characteristics and their contribution to microfiltration in submerged membrane bioreactors. *J. Membr. Sci.* **2003**, *216*, 217–227. [CrossRef]
42. Meng, F.; Chae, S.R.; Drews, A.; Kraume, M.; Shin, H.S.; Yang, F. Recent advances in membrane bioreactors (MBRs): Membrane fouling and membrane material. *Water Res.* **2009**, *43*, 1489–1512. [CrossRef] [PubMed]
43. Meng, F.; Zhang, H.; Yang, F.; Li, Y.; Xiao, J.; Zhang, X. Effect of filamentous bacteria on membrane fouling in submerged membrane bioreactor. *J. Membr. Sci.* **2006**, *272*, 161–168. [CrossRef]
44. Krzeminski, P. Activated Sludge Filterability and Full-Scale Membrane Bioreactor Operation. Ph.D. Thesis, Delft University of Technology, Delft, The Netherlands, 22 January 2013.
45. Azami, H.; Sarrafzadeh, M.H.; Mehrnia, M.R. Influence of sludge rheological properties on the membrane fouling in submerged membrane bioreactor. *Desalin. Water Treat.* **2011**, *34*, 117–122. [CrossRef]
46. Chang, I.S.; Kim, S.N. Wastewater treatment using membrane filtration—Effect of biosolids concentration on cake resistance. *Process Biochem.* **2005**, *40*, 1307–1314. [CrossRef]
47. Wang, Z.; Chu, J.; Song, Y.; Cui, Y.; Zhang, H.; Zhao, X.; Li, Z.; Yao, J. Influence of operating conditions on the efficiency of domestic wastewater treatment in membrane bioreactors. *Desalination* **2009**, *245*, 73–81. [CrossRef]

48. Radjenović, J.; Matošić, M.; Mijatović, I. Membrane bioreactor (MBR) as an advanced wastewater treatment technology. In *Handbook of Environmental Chemistry*; Springer: Berlin/Heidelberg, Germany, 2008; Volume 5, pp. 37–101.
49. Iorhemen, O.T.; Hamza, R.A.; Tay, J.H. Membrane bioreactor (MBR) technology for wastewater treatment and reclamation: Membrane fouling. *Membranes* **2016**, *6*, 33. [CrossRef] [PubMed]
50. Reid, E.; Liu, X.; Judd, S.J. Sludge characteristics and membrane fouling in full-scale submerged membrane bioreactors. *Desalination* **2008**, *219*, 240–249. [CrossRef]
51. Fan, F.; Zhou, H. Interrelated Effects of Aeration and Mixed Liquor Fractions on Membrane Fouling for Submerged Membrane Bioreactor Processes in Wastewater Treatment. *Environ. Sci. Technol.* **2007**, *41*, 2523–2528. [CrossRef] [PubMed]
52. Hernandez Rojas, M.E.; Van Kaam, R.; Schetrite, S.; Albasi, C. Role and variations of supernatant compounds in submerged membrane bioreactor fouling. *Desalination* **2005**, *17*, 95–107. [CrossRef]
53. Salazar-Peláez, M.L.; Morgan-Sagastume, J.M.; Noyola, A. Influence of hydraulic retention time on UASB post-treatment with UF membranes. *Water Sci. Technol.* **2011**, *64*, 2299–2305. [CrossRef] [PubMed]
54. Chen, R.; Nie, Y.; Hu, Y.; Miao, R.; Utashiro, T.; Li, Q.; Xu, M.; Li, Y.Y. Fouling behaviour of soluble microbial products and extracellular polymeric substances in a submerged anaerobic membrane bioreactor treating low-strength wastewater at room temperature. *J. Membr. Sci.* **2017**, *531*, 1–9. [CrossRef]
55. Jiang, T. Characterization and Modelling of Soluble Microbial Products in Membrane Bioreactors. Ph.D. Thesis, Ghent University, Gent, Belgium, 2007.
56. Xie, W.M.; Ni, B.J.; Sheng, G.P.; Seviour, T.; Yu, H.Q. Quantification and kinetic characterization of soluble microbial products from municipal wastewater treatment plants. *Water Res.* **2016**, *88*, 703–710. [CrossRef] [PubMed]
57. Deng, L.; Guo, W.; Ngo, H.H.; Zhang, J.; Liang, S.; Xia, S.; Zhang, Z.; Li, J. A comparison study on membrane fouling in a sponge-submerged membrane bioreactor and a conventional membrane bioreactor. *Bioresour. Technol.* **2014**, *165*, 69–74. [CrossRef] [PubMed]
58. Jørgensen, M.K.; Nierychlo, M.; Nielsen, A.H.; Larsen, P.; Christensen, M.L.; Nielsen, P.H. Unified understanding of physico-chemical properties of activated sludge and fouling propensity. *Water Res.* **2017**, *120*, 117–132. [CrossRef] [PubMed]
59. Van den Broeck, R.; Krzeminski, P.; Van Dierdonck, J.; Gins, G.; Lousada-Ferreira, M.; Van Impe, J.F.M.; van der Graaf, J.H.J.M.; Smets, I.Y.; van Lier, J.B. Activated sludge characteristics affecting sludge filterability in municipal and industrial MBRs: Unraveling correlations using multi-component regression analysis. *J. Membr. Sci.* **2011**, *378*, 330–338. [CrossRef]
60. Liu, Y.; Fang, H.H.P. Influences of extracellular polymeric substances (EPS) on flocculation, settling, and dewatering of activated sludge. *Crit. Rev. Environ. Sci. Technol.* **2003**, *33*, 237–273. [CrossRef]
61. Tu, X.; Zhang, S.; Xu, L.; Zhang, M.; Zhu, J. Performance and fouling characteristics in a membrane sequence batch reactor (MSBR) system coupled with aerobic granular sludge. *Desalination* **2010**, *261*, 191–196. [CrossRef]
62. Jang, N.; Ren, X.; Choi, K.; Kim, I.S. Comparison of membrane biofouling in nitrification and denitrification for the membrane bioreactor (MBR). *Water Sci. Technol.* **2006**, *53*, 43–49. [CrossRef] [PubMed]
63. Nittami, T.; Tokunaga, H.; Satoh, A.; Takeda, M.; Matsumoto, K. Influence of surface hydrophilicity on polytetrafluoroethylene flat sheet membrane fouling in a submerged membrane bioreactor using two activated sludges with different characteristics. *J. Membr. Sci.* **2014**, *463*, 183–189. [CrossRef]
64. Tian, Y.; Chen, L.; Zhang, S.; Cao, C.; Zhang, S. Correlating membrane fouling with sludge characteristics in membrane bioreactors: An especial interest in EPS and sludge morphology analysis. *Bioresour. Technol.* **2011**, *102*, 8820–8827. [CrossRef] [PubMed]
65. Rahimi, Y.; Torabian, A.; Mehrdadi, N.; Habibi-Rezaie, M.; Pezeshk, H.; Nabi-Bidhendi, G.R. Optimizing aeration rates for minimizing membrane fouling and its effect on sludge characteristics in a moving bed membrane bioreactor. *J. Hazard. Mater.* **2011**, *186*, 1097–1102. [CrossRef] [PubMed]
66. Delrue, F.; Stricker, A.E.; Mietton-Peuchot, M.; Racault, Y. Relationships between mixed liquor properties, operating conditions and fouling on two full-scale MBR plants. *Desalination* **2011**, *272*, 9–19. [CrossRef]
67. Wang, Z.; Wu, Z.; Tang, S. Impact of temperature seasonal change on sludge characteristics and membrane fouling in a submerged membrane bioreactor. *Sep. Sci. Technol.* **2010**, *45*, 920–927. [CrossRef]

68. Li, X.F.; Zhang, L.N.; Du, G.C. Influence of sludge discharge on sludge settleability and membrane flux in a membrane bioreactor. *Environ. Technol.* **2010**, *31*, 1289–1294. [CrossRef] [PubMed]
69. Kim, D.S.; Kang, J.S.; Lee, Y.M. The Influence of Membrane Surface Properties on Fouling in a Membrane Bioreactor for Wastewater Treatment. *Sep. Sci. Technol.* **2005**, *39*, 833–854. [CrossRef]
70. Gitis, V.; Rothenberg, G. *Ceramic Membranes: New Opportunities and Practical Applications*; Wiley-VCH Verlag GmbH & Co. KGaA: Weinheim, Germany, 2016; p. 394, ISBN 978-3-527-33493-3.
71. Iversen, V. Comprehensive Assessment of Flux Enhancers in Membrane Bioreactors for Wastewater Treatment. Ph.D. Thesis, Technical University of Berlin, Berlin, Germany, 4 October 2010.
72. Yonekawa, H.; Tomita, Y.; Watanabe, Y. Behavior of micro-particles in monolith ceramic membrane filtration with pre-coagulation. *Water Sci. Technol.* **2004**, *50*, 317–325. [CrossRef] [PubMed]
73. Dickhout, J.M.; Moreno, J.; Biesheuvel, P.M.; Boels, L.; Lammertink, R.G.H.; de Vos, W.M. Produced water treatment by membranes: A review from a colloidal perspective. *J. Colloid Interface Sci.* **2017**, *487*, 523–534. [CrossRef] [PubMed]
74. Jin, L.; Ong, S.L.; Ng, H.Y. Comparison of fouling characteristics in different pore-sized submerged ceramic membrane bioreactors. *Water Res.* **2010**, *44*, 5907–5918. [CrossRef] [PubMed]
75. Meabe, E.; Lopetegui, J.; Ollo, J.; Lardies, S. Ceramic Membrane Bioreactor: Potential applications and challenges for the future. In Proceedings of the MBR Asia International Conference, Kuala Lumpur, Malaysia, 25–26 April 2011.
76. Shi, X.; Tal, G.; Hankins, N.P.; Gitis, V. Fouling and cleaning of ultrafiltration membranes: A review. *J. Water Process Eng.* **2014**, *1*, 121–138. [CrossRef]
77. Wang, Z.; Ma, J.; Tang, C.Y.; Kimura, K.; Wang, Q.; Han, X. Membrane cleaning in membrane bioreactors: A review. *J. Membr. Sci.* **2014**, *468*, 276–307. [CrossRef]
78. Chen, F.; Bi, X.; Ng, H.Y. Effects of bio-carriers on membrane fouling mitigation in moving bed membrane bioreactor. *J. Membr. Sci.* **2016**, *499*, 134–142. [CrossRef]
79. Lee, S.J.; Dilaver, M.; Park, P.K.; Kim, J.H. Comparative analysis of fouling characteristics of ceramic and polymeric microfiltration membranes using filtration models. *J. Membr. Sci.* **2013**, *432*, 97–105. [CrossRef]
80. Larrea, A.; Rambor, A.; Fabiyi, M. Ten years of industrial and municipal membrane bioreactor (MBR) systems—Lessons from the field. *Water Sci. Technol.* **2014**, *70*, 279–288. [CrossRef] [PubMed]
81. Bérubé, P.R.; Hall, E.R.; Sutton, P.M. Parameters Governing Permeate Flux in an Anaerobic Membrane Bioreactor Treating Low-Strength Municipal Wastewaters: A Literature Review. *Water Environ. Res.* **2006**, *78*, 887–896. [CrossRef] [PubMed]
82. Lin, H.; Gao, W.; Meng, F.; Liao, B.-Q.; Leung, K.-T.; Zhao, L.; Chen, J.; Hong, H. Membrane Bioreactors for Industrial Wastewater Treatment: A Critical Review. *Crit. Rev. Environ. Sci. Technol.* **2012**, *42*, 677–740. [CrossRef]
83. Park, S.H.; Park, Y.G.; Lim, J.-L.; Kim, S. Evaluation of ceramic membrane applications for water treatment plants with a life cycle cost analysis. *Desalin. Water Treat.* **2015**, *54*, 973–979. [CrossRef]
84. Çiçek, N.; Franco, H.P.; Suidan, M.T.; Urbain, V.; Manem, J. Characterization and Comparison of a Membrane Bioreactor and a Conventional Activated-Sludge System in the Treatment of Wastewater Containing High-Molecular-Weight Compounds. *Water Environ. Res.* **1999**, *71*, 64–70. [CrossRef]
85. Shang, R.; Verliefde, A.R.D.; Hu, J.; Heijman, S.G.J.; Rietveld, L.C. The impact of EfOM, NOM and cations on phosphate rejection by tight ceramic ultrafiltration. *Sep. Purif. Technol.* **2014**, *132*, 289–294. [CrossRef]
86. Jeong, Y.; Kim, Y.; Jin, Y.; Hong, S.; Park, C. Comparison of filtration and treatment performance between polymeric and ceramic membranes in anaerobic membrane bioreactor treatment of domestic wastewater. *Sep. Purif. Technol.* **2018**, *199*, 182–188. [CrossRef]
87. Hofs, B.; Ogier, J.; Vries, D.; Beerendonk, E.F.; Cornelissen, E.R. Comparison of ceramic and polymeric membrane permeability and fouling using surface water. *Sep. Purif. Technol.* **2011**, *79*, 365–374. [CrossRef]
88. Jeong, Y.; Cho, K.; Kwon, E.E.; Tsang, Y.F.; Rinklebe, J.; Park, C. Evaluating the feasibility of pyrophyllite-based ceramic membranes for treating domestic wastewater in anaerobic ceramic membrane bioreactors. *Chem. Eng. J.* **2017**, *328*, 567–573. [CrossRef]
89. Jeong, Y.; Lee, S.; Hong, S.; Park, C. Preparation, characterization and application of low-cost pyrophyllite-alumina composite ceramic membranes for treating low-strength domestic wastewater. *J. Membr. Sci.* **2017**, *536*, 108–115. [CrossRef]

90. Kaniganti, C.M.; Emani, S.; Thorat, P.; Uppaluri, R. Microfiltration of Synthetic Bacteria Solution Using Low Cost Ceramic Membranes. *Sep. Sci. Technol.* **2015**, *50*, 121–135. [CrossRef]
91. Li, L.; Chen, M.; Dong, Y.; Dong, X.; Cerneaux, S.; Hampshire, S.; Caoa, J.; Zhua, L.; Zhua, Z.; Liu, J. A low-cost alumina-mullite composite hollow fiber ceramic membrane fabricated via phase-inversion and sintering method. *J. Eur. Ceram. Soc.* **2016**, *36*, 2057–2066. [CrossRef]
92. Lorente-ayza, M.; Pérez-fernández, O.; Alcalá, R.; Sánchez, E.; Mestre, S.; Coronas, J.; Menéndez, M. Comparison of porosity assessment techniques for low-cost ceramic membranes. *Boletín de La Sociedad Española de Cerámica Y Vidrio* **2017**, *56*, 29–38. [CrossRef]
93. Tewari, P.K.; Singh, R.K.; Batra, V.S.; Balakrishnan, M. Membrane bioreactor (MBR) for wastewater treatment: Filtration performance evaluation of low cost polymeric and ceramic membranes. *Sep. Purif. Technol.* **2010**, *71*, 200–204. [CrossRef]
94. Chemometric Analysis for Spectroscopy. Available online: http://www.camo.com/downloads/resources/application_notes/Chemometric%20Analysis%20for%20Spectroscopy.pdf (accessed on 19 July 2018).
95. Singh, K.P.; Malik, A.; Mohan, D.; Sinha, S.; Singh, V.K. Chemometric data analysis of pollutants in wastewater—A case study. *Anal. Chim. Acta* **2005**, *532*, 15–25. [CrossRef]
96. Torgersen, G.; Rød, J.K.; Kvaal, K.; Bjerkholt, J.T.; Lindholm, O.G. Evaluating flood exposure for properties in Urban areas using a multivariate modelling technique. *Water* **2017**, *9*, 318. [CrossRef]
97. Philippe, N.; Racault, Y.; Stricker, A.E.; Spérandio, M.; Vanrolleghem, P.A. Modelling the long-term evolution of permeability in full-scale municipal MBRs: A multivariate statistical modelling approach. *Procedia Eng.* **2012**, *44*, 574–580. [CrossRef]
98. Kaneko, H.; Funatsu, K. Visualization of Models Predicting Transmembrane Pressure Jump for Membrane Bioreactor. *Ind. Eng. Chem. Res.* **2012**, *51*, 9679–9686. [CrossRef]
99. De Temmerman, L.; Naessens, W.; Maere, T.; Marsili-Libelli, S.; Villez, K.; Nopens, I.; Temmink, H.; Nopens, I. Detecting membrane fouling occurrences in a full-scale membrane bioreactor with principal component analysis. In Proceedings of the 11th IWA Conference on Instrumentation Control and Automation (ICA), Narbonne, France, 18–20 September 2013.
100. Ji, J.; Qiu, J.; Wong, F.; Li, Y. Enhancement of filterability in MBR achieved by improvement of supernatant and floc characteristics via filter aids addition. *Water Res.* **2008**, *42*, 3611–3622. [CrossRef] [PubMed]
101. Wu, J.; Huang, X. Use of ozonation to mitigate fouling in a long-term membrane bioreactor. *Bioresour. Technol.* **2010**, *101*, 6019–6027. [CrossRef] [PubMed]
102. Todt, D.; Heistad, A.; Jenssen, P.D. Load and distribution of organic matter and nutrients in a separated household wastewater stream. *Environ. Technol.* **2015**, *36*, 1584–1593. [CrossRef] [PubMed]
103. Ying, Z.; Ping, G. Effect of powdered activated carbon dosage on retarding membrane fouling in MBR. *Sep. Purif. Technol.* **2006**, *52*, 154–160. [CrossRef]
104. Judd, S. The status of membrane bioreactor technology. *Trends Biotechnol.* **2008**, *26*, 109–116. [CrossRef] [PubMed]
105. Rosenberg, M.; Gutnick, D.; Rosenberg, E. Adherence of bacteria to hydrocarbons: A simple method for measuring cell-surface hydrophobicity. *FEMS Microbiol. Lett.* **1980**, *9*, 29–33. [CrossRef]
106. Effect of MLSS on Flux—MLSS Paradox. Available online: http://onlinembr.info/membrane-process/effect-of-mlss-on-flux-mlss-paradox/ (accessed on 22 January 2018).
107. Brookes, A.; Judd, S.; Reid, E.; Germain, E.; Smith, S.; Alvarez-Vazquez, H.; Le-Clech, P.; Stephenson, T.; Turra, E.; Jefferson, B. Biomass characterisation in membrane bioreactors. In Proceedings of the International Membrane Science and Technology Conference (IMSTEC), Sydney, Australia, 10–14 November 2003.
108. Jefferson, B.; Brookes, A.; Le-Clech, P.; Judd, S.J. Methods for understanding organic fouling in MBRs. *Water Sci. Technol.* **2004**, *49*, 237–244. [CrossRef] [PubMed]
109. Huang, X.; Wu, J. Improvement of membrane filterability of the mixed liquor in a membrane bioreactor by ozonation. *J. Membr. Sci.* **2008**, *318*, 210–216. [CrossRef]
110. Chae, S.R.; Ahn, Y.T.; Kang, S.T.; Shin, H.S. Mitigated membrane fouling in a vertical submerged membrane bioreactor (VSMBR). *J. Membr. Sci.* **2006**, *280*, 572–581. [CrossRef]
111. Ng, H.Y.; Hermanowicz, S.W. Membrane bioreactor operation at short solids retention times: Performance and biomass characteristics. *Water Res.* **2005**, *39*, 981–992. [CrossRef] [PubMed]
112. Fan, F.; Zhou, H.; Husain, H. Identification of wastewater sludge characteristics to predict critical flux for membrane bioreactor processes. *Water Res.* **2006**, *40*, 205–212. [CrossRef] [PubMed]

113. Wu, J.; Huang, X. Effect of mixed liquor properties on fouling propensity in membrane bioreactors. *J. Membr. Sci.* **2009**, *342*, 88–96. [CrossRef]
114. Lee, W.-N.; Chang, I.-S.; Hwang, B.-K.; Park, P.-K.; Lee, C.-H.; Huang, X. Changes in biofilm architecture with addition of membrane fouling reducer in a membrane bioreactor. *Process Biochem.* **2007**, *42*, 655–661. [CrossRef]
115. Kunacheva, C.; Stuckey, D. Analytical methods for soluble microbial products (SMP) and extracellular polymers (ECP) in wastewater treatment systems: A review. *Water Res.* **2014**, *61*, 1–18. [CrossRef] [PubMed]
116. Lesjean, B.; Rosenberger, S.; Laabs, C.; Jekel, M.; Gnirss, R.; Amy, G. Correlation between membrane fouling and soluble/colloidal organic substances in membrane bioreactors for municipal wastewater treatment. *Water Sci. Technol.* **2005**, *51*, 1–8. [CrossRef] [PubMed]
117. CAMO. *The Unscrambler, Tutorials CAMO Process AS 2006*; CAMO Software AS: Oslo, Norway, 2006.
118. Deng, L.; Guo, W.; Hao Ngo, H.; Zhang, H.; Wang, J.; Li, J.; Xia, S.; Wu, Y. Biofouling and control approaches in membrane bioreactors. *Bioresour. Technol.* **2016**, *221*, 656–665. [CrossRef] [PubMed]
119. Isma Aida, M.I.; Idris, A.; Omar, R.; Razreena Putri, A.R. Effects of SRT and HRT on Treatment Performance of MBR and Membrane Fouling. *Int. J. Chem. Mol. Nucl. Mater. Metall. Eng.* **2014**, *8*, 488–492.
120. Van den Broeck, R.; Van Dierdonck, J.; Nijskens, P.; Dotremont, C.; Krzeminski, P.; van der Graaf, J.H.J.M.; van Lier, J.B.; Van Impe, J.F.M.; Smets, I.Y. The influence of solids retention time on activated sludge bioflocculation and membrane fouling in a membrane bioreactor (MBR). *J. Membr. Sci.* **2012**, *401–402*, 48–55. [CrossRef]
121. Yigit, N.O.; Harman, I.; Civelekoglu, G.; Koseoglu, H.; Cicek, N.; Kitis, M. Membrane fouling in a pilot-scale submerged membrane bioreactor operated under various conditions. *Desalination* **2008**, *231*, 124–132. [CrossRef]
122. Malamis, S.; Andreadakis, A. Fractionation of proteins and carbohydrates of extracellular polymeric substances in a membrane bioreactor system. *Bioresour. Technol.* **2009**, *100*, 3350–3357. [CrossRef] [PubMed]
123. Sivchenko, N.; Kvaal, K.; Ratnaweera, H. Evaluation of image texture recognition techniques in application to wastewater coagulation. *Cogent Eng.* **2016**, *3*. [CrossRef]
124. Jiang, T.; Kennedy, M.D.; Guinzbourg, B.F.; Vanrolleghem, P.A.; Schippers, J.C. Optimising the operation of a MBR pilot plant by quantitative analysis of the membrane fouling mechanism. *Water Sci. Technol.* **2005**, *51*, 19–25. [CrossRef] [PubMed]
125. Le Clech, P.; Jefferson, B.; Chang, I.S.; Judd, S.J. Critical flux determination by the flux-step method in a submerged membrane bioreactor. *J. Membr. Sci.* **2003**, *227*, 81–93. [CrossRef]
126. Ognier, S.; Wisniewski, C.; Grasmick, A. Membrane bioreactor fouling in sub-critical filtration conditions: A local critical flux concept. *J. Membr. Sci.* **2004**, *229*, 171–177. [CrossRef]
127. Miller, D.J.; Kasemset, S.; Paul, D.R.; Freeman, B.D. Comparison of membrane fouling at constant flux and constant transmembrane pressure conditions. *J. Membr. Sci.* **2014**, *454*, 505–515. [CrossRef]